

Note

The microchannel flow model under shear stress and higher frequencies

K J Parker

Department of Electrical and Computer Engineering, University of Rochester,
Hopeman Building 203, PO Box 270126, Rochester, NY 14627-0126,
United States of America

E-mail: kevin.parker@rochester.edu

Received 29 November 2016

Accepted for publication 24 February 2017

Published 21 March 2017



CrossMark

Abstract

The microchannel flow model provides a framework for considering the effect of the vascular bed on the time domain and frequency domain response of soft tissues. The derivation originates with a single small fluid-filled vessel in an elastic medium under uniaxial compression. A fractal branching vasculature is also assumed to be present in the tissue under consideration. This note considers two closely related issues. First, the response of the element under compression or shear as a function of the orientation of the fluid-filled vessel is considered. Second, the transition from quasistatic (Poiseuille's Law) to dynamic (Womersley equations) fluid flow is examined to better predict the evolution of behavior at higher frequencies. These considerations expand the conceptual framework of the microchannel flow model, particularly the range and limits of validity.

Keywords: rheology, biomechanics, elastography, shear waves

(Some figures may appear in colour only in the online journal)

1. Introduction

The microchannel flow model (MFM) is derived from consideration of the outflow of fluid from a small vessel during uniaxial compression. A key relationship stems from the use of Poiseuille's Law and the assumption of a power law (fractal) distribution of vessel sizes in the continuous limit. Two concerns about the applicability of this model to shear wave dispersion experiments in tissue have been raised by astute colleagues (personal communication, Carstensen and Mc Aleavey (2015)). First, the use of the MFM model for shear waves in tissues assumes the relationship that shear modulus $G = E/3$. This is valid for isotropic materials near the incompressible limit, but requires re-examination in the case of a vascularized

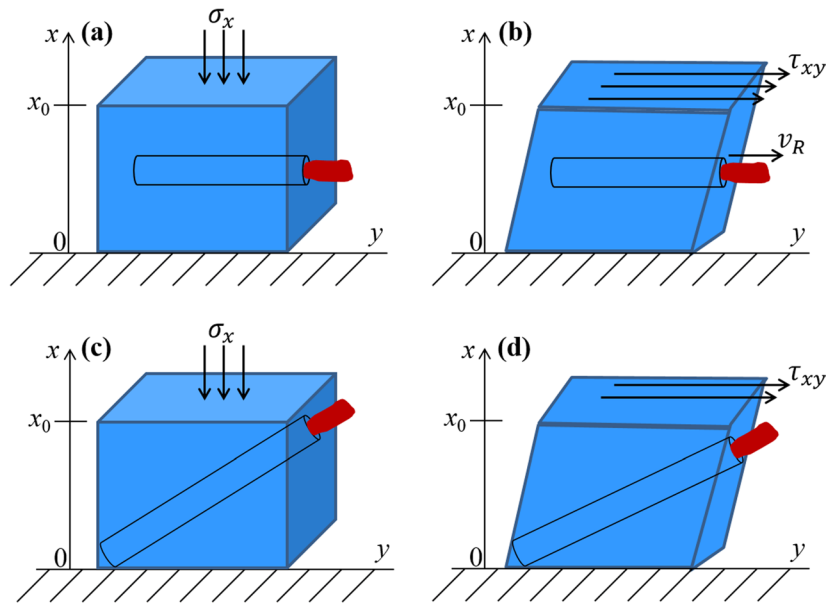


Figure 1. Elastic element with single vessel in uniaxial compression (a) or shear (b). In (c) and (d) the microchannel is oriented near the diagonal.

tissue. Secondly, the MFM model derivation begins with a uniaxial compression, whereas shear wave experiments in tissue involve rotational, divergence-free, or equi-voluminal waves (Graff 1975). In addition, the dependency on vessel orientation has not been explicitly stated, nor has the limit at which inertial terms become non-negligible. These important concerns suggest a second look at the derivations of the MFM, considering an element in shear. These are examined in this note.

2. Theory

2.1. The basic model

Consider an idealized block of tissue in figure 1 comprised of a purely elastic isotropic material and a single small vessel, or microchannel, containing fluid. Its action under uniaxial compression (a) results in loss of fluid volume and a corresponding component of strain.

Using Poiseuille's Law to account for the fluid outflow, we previously derived as a first approximation one component of strain ε_x due to outflow of fluid (Parker 2014):

$$\sigma_x = \eta \left(\frac{A_0 x_0}{C r^4} \right) \frac{d\varepsilon_x}{dt}, \quad (1)$$

which is essentially a dashpot equation where σ_x is the stress, η is the viscosity of the fluid, r is the radius of the vessel, $A_0 x_0$ is the volume of the cube, and C is a constant.

By combining this with the elastic response of the block element and applying superposition over all generations of vessel sizes we arrive at the final MFM frequency domain complex modulus derived in Parker (2014). For a comparison, we seek an alternative derivation using shear and will examine the relationship for similarities.

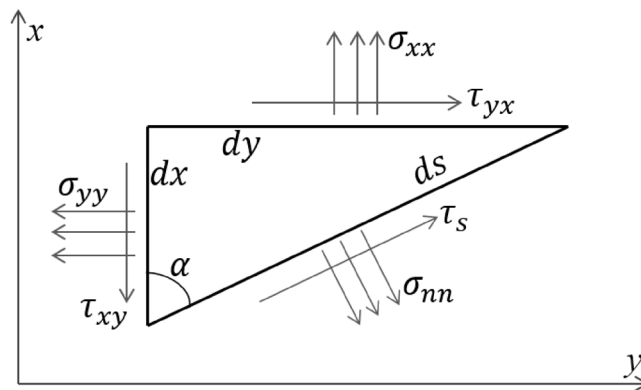


Figure 2. 2D stress transformation diagram where the angle α is measured from the vertical (x) axis.

2.2. Angle dependence of microvessel

Consider the case of figure 1(c) where uniaxial stress is applied but the microchannel is oriented approximately on the diagonal. For simplicity we use the general relations of 2D stress transformation (Shames 1967) (figure 2),

$$\sigma_{nn} = \left(\frac{\sigma_{xx} + \sigma_{yy}}{2} \right) + \left(\frac{\sigma_{yy} - \sigma_{xx}}{2} \cos 2\alpha \right) + (\tau_{xy} \sin 2\alpha). \quad (2)$$

Assuming the element of figure 1(c) is small and only σ_{xx} is non-zero then with $\alpha = 45^\circ$ as the angle of the microchannel, the stress normal to the channel boundary is $\sigma_{nn} = \sigma_{xx}/2$. Assuming negligible flow and low frequency (quasistatic) response, a vessel oriented at angle α would have a normal stress on the vessel reduced by a factor of $(1 - \cos 2\alpha)/2$ or, equivalently, $\sin^2(\alpha)$ from the original case (figure 1(a)) but otherwise the derivation of the MFM would proceed as before (Parker 2014).

2.3. The element in shear

Consider the elements shown in figures 1(b) and (d) where τ_{xy} is applied on the top surface and all other applied stresses are zero. The transformation of normal stress depends on angle α as $\sin 2\alpha$. For the microvessel at $\alpha = 45^\circ$ in figure 1(d) the normal stress σ_{nn} will be:

$$\sigma_{nn} = \tau_{xy}(\sin 90^\circ) = \tau_{xy}. \quad (3)$$

Thus, a normal stress exists on the vessel boundaries resulting in an internal pressure and the derivation of the MFM continues as before. For $\alpha = 90^\circ$, case 1(b), there is no stress normal to the vessel boundary. In tissues with numerous vessels, the macroscopic effects of this angle dependence would be observable (or not) depending on the statistical anisotropy (or isotropy) of orientation of the microvessel in specific tissues.

2.4. The transition from quasistatic to dynamic behavior

Consider next element of figures 1(a), (c) and (d), where forces are applied sinusoidally at frequency ω . The key derivations for sinusoidal fluid behavior in pipes are related to the seminal works by Hale *et al* (1955) and Womersley (1955, 1957), who considered the velocity, flow, pressure, and drag relationships in sinusoidal steady state, for laminar flow.

Womersley’s solution pertains to a stationary pipe with a sinusoidal pressure gradient $(\Delta P/L)\mathbf{e}^{i\omega t}$ applied across some length L at frequency ω . In the case of the elements of figures 1(a), (c) and (d), we assume that the normal stress field $\sigma_{xx}\mathbf{e}^{i\omega t}$ acting on the center of the element creates a sinusoidal pressure gradient along the vessels, since the external faces of the unconfined element have $P = 0$.

In this case, assuming $\frac{\Delta P}{L} \approx \frac{\sigma_{xx}}{x_0}$, Womersley’s solution for fluid velocity v is:

$$v(r, t) = \text{Re} \left[\left(\frac{J_0 \left[(-1)^{3/4} r \sqrt{\frac{\omega}{\nu}} \right]}{J_0 \left[(-1)^{3/4} R \sqrt{\frac{\omega}{\nu}} \right]} - 1 \right) \frac{i\sigma_{xx}\mathbf{e}^{i\omega t}}{x_0\omega\rho} \right], \tag{4}$$

where ν is the coefficient of kinematic viscosity (μ/ρ), μ is the dynamic viscosity, and ρ is the density. The viscous drag on the walls of the vessel is:

$$F = -2\pi\mu x_0 R \left. \frac{dv}{dr} \right|_{r=R} = \text{Re} \left[\left(\frac{(-1)^{1/4} \sigma_{xx} \mathbf{e}^{i\omega t} (-2\pi\mu R)}{\sqrt{\omega\nu}\rho} \right) \left(\frac{J_1 \left[(-1)^{3/4} R \sqrt{\frac{\omega}{\nu}} \right]}{J_0 \left[(-1)^{3/4} R \sqrt{\frac{\omega}{\nu}} \right]} \right) \right]. \tag{5}$$

Taking a series expansion of this in terms of ω about the function at $\omega = 0$, this yields

$$F(\omega) \cong \sigma_{xx}\pi R^2 - \frac{\sigma_{xx}\pi R^6 \omega^2}{48\nu^2} + \text{h.o.t.} \tag{6}$$

The first term is a static term consistent with Poiseuille’s law. The second term is the inertial term, which dominates when $\omega^2 > (48\nu^2/R^4)$ or approximately:

$$\omega > 7(\nu/R^2). \tag{7}$$

We note the strong $1/R^2$ dependence on the transition to significant inertial terms.

If we take the $\nu_{\text{blood}} = 4 \times 10^6 \text{ m}^2 \text{ s}^{-1}$, and $R = 0.1 \text{ mm} = 1 \times 10^{-4} \text{ m}$ (the size associated with secondary and tertiary arterial branches (McDonald 1974, Zamir and Phipps 1988)), then $\omega > 7 \left(\frac{4 \times 10^{-6}}{1 \times 10^{-8}} \right) = 2800 \text{ rad s}^{-1}$, or 445 Hz, in the upper range of many acoustic radiation force pulse propagation spectra.

Alternatively, in the case of figure 1(b), the vessel walls are oscillating with the elastic element and the fluid is responding with no applied internal or external pressure gradient. Let the vessel wall velocity be

$$v(R) = v_0 \mathbf{e}^{i\omega t} \quad \text{at} \quad r = R. \tag{8}$$

The governing differential equation for the fluid is (Zhdanov and Kasemo 2015):

$$\frac{\partial v}{\partial t} = \frac{\nu}{r} \frac{\partial}{\partial r} \left(r \frac{\partial v}{\partial r} \right). \tag{9}$$

The solution is

$$v(r, t) = \text{Re} \left[v_0 \left(\frac{J_0 \left[(-1)^{3/4} r \sqrt{\frac{\omega}{\nu}} \right]}{J_0 \left[(-1)^{3/4} R \sqrt{\frac{\omega}{\nu}} \right]} \right) \mathbf{e}^{i\omega t} \right] \tag{10}$$

The total drag of the fluid on the pipe is given by

$$F = -2\pi\mu R x_0 \left. \frac{dv}{dr} \right|_{r=R}, \quad (11)$$

and therefore

$$F = \left(\frac{v_0 \cdot 2\pi\mu R x_0 (-1)^{3/4} J_1 \left[(-1)^{3/4} R \sqrt{\frac{\omega}{v}} \right]}{J_0 \left[(-1)^{3/4} R \sqrt{\frac{\omega}{v}} \right]} \right) \left(\sqrt{\frac{\omega}{v}} \right). \quad (12)$$

Expanding in a power series of ω around $\omega = 0$ yields:

$$F \cong -i\rho\pi R^2 v_0 \omega x_0, \quad (13)$$

however $v_0 = i\omega(\xi \cdot x_0)$ where ξ is the shear strain τ_{xy}/G and G is the shear modulus. Thus,

$$F \cong + \left(\rho\pi R^2 \frac{\tau_{xy}}{G} x_0^2 \right) \omega^2. \quad (14)$$

The force applied at the surface of the element is $\tau_{xy} x_0^2$. Arbitrarily choosing a 1% ratio of forces (inertial/applied) as the level at which the inertial term becomes important:

$$\begin{aligned} \omega^2 \left(\rho\pi R^2 \frac{\tau_{xy}}{G} x_0^2 \right) &> 0.01 (\tau_{xy} x_0^2) \\ \omega^2 &> 0.01 \left(\frac{G}{\rho\pi R^2} \right). \end{aligned} \quad (15)$$

Choosing $R = 1 \times 10^{-4}$ m, $\rho = 1 \times 10^3$ kg m⁻³, $G = 10 \times 10^3$ Pa = 10×10^3 kg (m · s⁻²)⁻¹:

$$\omega > 0.1 \sqrt{\frac{10 \times 10^3}{(1 \times 10^3)(1 \times 10^{-4})^2}} > 3160 \text{ rad s}^{-1}, \quad (16)$$

or $f > 500$ Hz, consistent with the previous analysis of the configurations shown in figures 1(a), (c) and (d).

3. Discussion

We considered four cases of an idealized block of tissue with a single microvessel, in uniaxial compression and in pure shear, and with horizontal and diagonal orientations of the microvessel. The applied stresses will create a stress on the vessel and initiate flow; however there is a directional dependency of $\sin 2\alpha$ in the cases where shear is applied (figures 1(b) and (d)), and a dependency of $(1 - \cos 2\alpha)/2$ for uniaxial compression (figures 1(a) and (c)). Measurements of tissues will typically capture an ensemble of vessels over a range of orientations. In some soft vascularized tissues and tumors, there is no strong directional orientation of the vascular tree at the level of a millimeter. In these cases of statistical isotropy of directionality, the same shear wave or stress relaxation responses will be seen independent of the orientation of the applied stresses. However, the possibility exists for measureable directional dependence in tissues where a strong spatial directionality of microvessels is present.

The transition from quasistatic to high frequency behavior was also examined for cases where an oscillating pressure gradient drives the flow (Womersley's solution) and the case where pure shear motion of the vessel walls drives the oscillatory flow. In both cases the

solution for an arteriole of radius 0.1 mm suggests that shear wave frequencies of greater than 500 Hz would require additional inertial terms beyond the MFM solution. This compares rather closely to the landmark paper on waves in porous rocks by Biot (1956), where he says that ‘the assumption of Poiseuille flow breaks down if the frequency exceeds a certain value’. He then suggests that ‘For a porous material we may assume that the Poiseuille flow breaks down when this quarter wavelength is of the order of the diameter d of the pores’. Then, in an example using water between parallel plates separated by 0.1 mm, he finds a limiting frequency of 100 Hz. If we simply apply a factor of 5 for the shear viscosity of blood compared to water (Ozbek 1971, Stammers *et al* 2003), this converts to 500 Hz for the same dimension, which is the transition frequency found in the analyses of section 2 (Theory) of this paper. Thus, our results are in agreement with the landmark findings of Biot, despite the very different approaches taken.

However, the situation in tissues is not simple since there is no single ‘pore’ size, rather a distribution of characteristic dimensions of the fractal branching vasculature and other micro-channel spaces, and our analysis shows explicitly the dependence of the high frequency transition on vessel radius. For example, the larger arteries and veins will transition to a high frequency (Womersley as opposed to Poiseuille) behavior at relatively low frequencies, as shown by equations (7) and (15). In elastography experiments using clinical magnetic resonance and ultrasound scanners, major vessels are typically excluded from analyses, thus the attention to sub-millimeter diameters as key drivers of ensemble averaged behavior is appropriate.

4. Conclusion

We examined the simple model of an elastic block in either uniaxial compression or shear, where a single fluid-filled vessel is oriented at different angles. Some commonalities emerge but the details are distinct. Both the compression and shear cases will experience a relaxation associated with fluid outflow from the vessel. However in the case of compression, the normal stress on the vessel walls varies as $(1 - \cos 2\alpha)/2$, where α is the angle of the vessel orientation with respect to the x -axis, whereas in the case of shear the normal stress on the vessel walls varies as $\sin 2\alpha$. Thus, the peak effect is seen at 90° (figure 1(a)) for uniaxial x -compression, and 45° (figure 1(d)) for shear.

Another important issue concerns the transition from quasistatic to dynamic solutions, and at what frequency range the dynamic or inertial terms will become important. By applying classical solutions related to Womersley derivations, we identify 500 Hz as a transition frequency within the tertiary arterial branches; however, the strong dependence on vessel radius makes a more general statement about tissue as a whole difficult to make, since the range of vessel diameters is broad. Further research is required to incorporate the effect of the entire range of vascularity as a function of frequency and in cases of strong vascular anisotropy.

Acknowledgments

This work was supported by the Hajim School of Engineering and Applied Sciences at the University of Rochester. Professor Sheryl Gracewski is gratefully acknowledged for insightful comments and suggestions. We are deeply indebted to the late Professor Edwin Carstensen for his keen insights and deep questions which motivated this research.

References

- Biot M A 1956 Theory of propagation of elastic waves in a fluid-saturated porous solid. I. Low-frequency range *J. Acoust. Soc. Am.* **28** 168–78
- Carstensen E and Mc Aleavey S 2015 ed K J Parker personal communication
- Graff K F 1975 *Wave Motion in Elastic Solids* (Oxford: Clarendon Press)
- Hale J F, Mc D D and Womersley J R 1955 Velocity profiles of oscillating arterial flow, with some calculations of viscous drag and the Reynolds numbers *J. Physiol.* **128** 629–40
- McDonald D A 1974 *Blood Flow in Arteries* (London: Edward Arnold)
- Ozbek H 1971 Viscosity of aqueous sodium chloride from 0 to 150 °C *American Chemical Society 29th Southeast Regional Meeting (Tampa, FL)* pp 1–67
- Parker K J 2014 A microchannel flow model for soft tissue elasticity *Phys. Med. Biol.* **59** 4443–57
- Shames I H 1967 *Engineering Mechanics; Statics and Dynamics* (Englewood Cliffs, NJ: Prentice-Hall) ch 9 p xviii 748 p
- Stammers A H, Vang S N, Mejak B L and Rauch E D 2003 Quantification of the effect of altering hematocrit and temperature on blood viscosity *J. Extra Corpor. Technol.* **35** 143–51
- Womersley J R 1955 Method for the calculation of velocity, rate of flow and viscous drag in arteries when the pressure gradient is known *J. Physiol.* **127** 553–63
- Womersley J R 1957 Oscillatory flow in arteries: the constrained elastic tube as a model of arterial flow and pulse transmission *Phys. Med. Biol.* **2** 178
- Zamir M and Phipps S 1988 Network analysis of an arterial tree *J. Biomech.* **21** 25–34
- Zhdanov V P and Kasemo B 2015 Liquid in a tube oscillating along its axis *Physica E* **70** 35–9